ELSEVIER

Chemical Physics 281 (2002) 465–476

Chemical Physics

www.elsevier.com/locate/chemphys

Fingerprints of mesoscopic leads in the conductance of a molecular wire

Gianaurelio Cuniberti[a,*], Giorgos Fagas[a,b], Klaus Richter[b]

[a] *Max Planck Institute for the Physics of Complex Systems, Nöthnitzer Strasse 38, D-01187 Dresden, Germany*
[b] *Institute for Theoretical Physics, University of Regensburg, D-93040 Regensburg, Germany*

Received 2 November 2001

Abstract

The influence of contacts on linear transport through a molecular wire attached to mesoscopic tubule leads is studied. It is shown that low dimensional leads, such as carbon nanotubes, in contrast to bulky electrodes, strongly affect transport properties.

By focusing on the specificity of the lead-wire contact, we show, in a fully analytical treatment, that the geometry of this hybrid system supports a mechanism of channel selection and a sum rule, which is a distinctive hallmark of the mesoscopic nature of the electrodes.

Keywords: Carbon nanotubes; Electronic transport; Green functions

1. Introduction

Future electronic miniaturization may enter a regime where devices are dominated by quantum mechanical laws and eventually reach the single-molecule scale [1]. Although molecular materials for electronics have already been realized [2], their implementation in real applications [3–5] still has to cope with challenges in utilization, synthesis, and assembly [6]. Concerning theoretical ideas and methods the problem is also two-sided: on the one hand many theoretical ideas are already footed on past pioneering work, such as the proposal of molecular rectification in 1974 [7] which was experimentally realized only 20 years later [8]. On the other hand most of the conventional methods frequently employed for characterizing transport properties in microelectronic devices, such as the Boltzmann equation, can no longer be applied at the molecular scale. Here conductance properties have to be calculated by employing full quantum mechanical approaches and by including the electronic structure of the molecules involved.

Electron transport on the atomic and molecular scale became a topic of intense investigation since the invention of the scanning tunneling microscope (STM). More recently, studies of transmission properties of single molecular junctions contacted

* Corresponding author. Tel.: +49-351-871-2213; fax: +49-351-871-1999.
E-mail address: cunibert@mpipks-dresden.mpg.de (G. Cuniberti).

0301-0104/02/$ - see front matter
PII: S0301-0104(02)00341-5

to metallic leads [9,10] have intensified the interest in the basic mechanisms of conduction across molecular bridges. The archetype of such a molecular device can be viewed as a donor and acceptor lead coupled by a molecule acting as a bridge. In such systems the traditional picture of electron transfer between donor and acceptor species is re-read in terms of a novel view in which a molecule can bear an electric current [11]. Molecular bridges have been realized out of single organic molecules [9,12], short DNA strands [10], but also as atomic wires [13–15]. Generally, contact effects alter the "intrinsic conductance" of the molecules in such experiments and call for closer theoretical studies.

In a parallel development the use of carbon nanotube (CNT) conductors has been the focus of intense experimental and theoretical activity as another promising direction for building blocks of molecular-scale circuits [16,17]. CNTs exhibit a wealth of properties depending on their diameter, orientation of graphene roll up, and on their topology, namely whether they consist of a single cylindrical surface (single-wall) or many surfaces (multi-wall) [18]. If CNTs are attached to other materials to build elements of molecular circuits, the characterization of contacts [19,20] becomes again a fundamental issue. This problem arises also when a CNT is attached to another *molecular wire*, a single molecule or a molecular cluster with a privileged direction of the current flow.

In the usual theoretical treatment of transport through molecular wires, the attached leads are approximated by a continuum of free or quasi-free states, mimicking the presence of large reservoirs provided by bulky electrodes. However such an assumption may become inadequate when considering leads with lateral dimensions of the order of the bridged molecule, as for CNTs [19]. The latter have been recently used as wiring elements [17], as active devices [17,21], and, attached to STM tips, for enhancing their resolution [22,23]. With a similar arrangement the fine structure of a twinned DNA molecule has been observed [24]. However, CNT-STM images seem to strongly depend on the tip shape and nature of contact with the imaging substrate [25]. This calls for a better characterization of the contact chemistry of such hybrid structures.

This paper addresses the influence of the molecular wire–electrode contacts on the linear conductance when the spectral structure and the geometry of the electrodes plays an important rôle. This allows us to quantify to which extent *mesoscopic leads* may affect the conductance. Owing to the relevance of CNT-based devices, we focus on bridges between tubular leads. In previous density-functional-theory-based treatments the conductance through systems such as a C_{60} molecule in between two CNTs has been calculated with high accuracy [26]. These numerical approaches showed a strong sensitivity of the current on the system geometries and strength of the molecule–CNT couplings.

In the present paper we focus on such contact effects. As a simple model for an atomic or molecular bridge we use a homogeneous linear chain which enables us to derive analytical expressions for the conductance in a non-interacting electron approximation. In addition, we implicitly assume that no significant charge is transferred between the leads and the molecular bridge at equilibrium since this could lead to an electrostatic potential-induced inhomogeneity [27]. The latter may hold for an all-carbon [26] structure and makes it possible to investigate the properties of our model in the whole parameter space. The system exhibits distinct transport features depending on the number and strength of contacts between the molecular bridge and the interface as well as on the symmetry of the channel wave functions transverse to the transport direction. Our findings, which are common for leads with tube topology, are then studied in detail for CNT leads (Fig. 1) by analytically treating the single-particle Green function. In particular, we demonstrate on the one hand that configurations with only one molecule–lead contact activated give rise to complex conductance spectra exhibiting quantum features of both the molecule and the electrodes; on the other hand multiple contacts provide a mechanism for transport channel selection leading to a regularization of the conductance, entirely provided by topological arguments. Channel selection particularly highlights the rôle of molecular resonant states by suppressing details assigned to the electrodes.

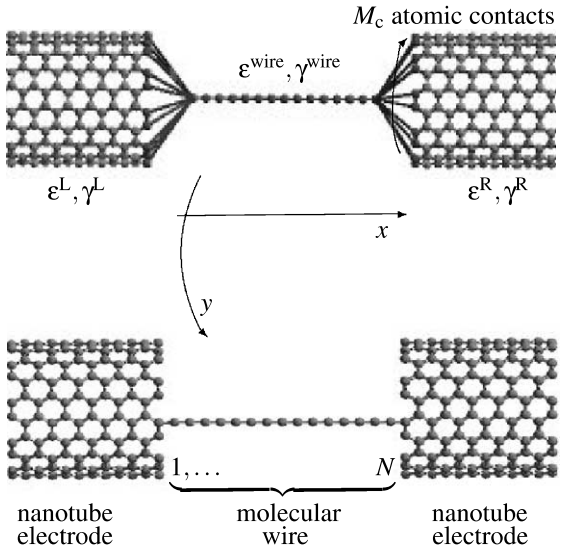

Fig. 1. Schematic representation of the molecular wire–CNT hybrid with single (bottom) and multiple (top) contacts. On-site energies $\varepsilon^{\alpha=L,R,wire}$ are chosen to be zero.

2. System and method

In a tight-binding description, the hamiltonian of the entire system, $H = H_{tubes} + H_{wire} + H_{coupling}$, reads

$$H = \sum_{\alpha=L,R,wire} \sum_{n_\alpha, n'_\alpha} t^\alpha_{n_\alpha, n'_\alpha} c^{\alpha\dagger}_{n_\alpha} c^\alpha_{n'_\alpha} - \sum_{m_L \leqslant M_c} \Gamma_{m_L} \left(c^{L\dagger}_{m_L} c^{wire}_1 + \text{h.c.} \right) - \sum_{m_R \leqslant M_c} \Gamma_{m_R} \left(c^{R\dagger}_{m_R} c^{wire}_N + \text{h.c.} \right). \quad (1)$$

Here, the matrix element $t^\alpha_{n_\alpha, n'_\alpha} = \varepsilon^\alpha_{n_\alpha} \delta_{n_\alpha, n'_\alpha} - \gamma^\alpha_{\langle n_\alpha, n'_\alpha \rangle}$ contains the on-site energy of each of the $n_{wire} = 1, \ldots, N$ chain-atoms, ε^{wire}, the orbital energy relative to that of the lead atoms, $\varepsilon^{L,R}$, and $\gamma^{L,R}$, γ^{wire}, and Γ are nearest neighbour hopping terms between atoms of the left or right leads, molecular bridge, and the bridge/lead interface, respectively. Note that $n_{L,R}$ is a two-dimensional coordinate spanning the tube lattice. Summations over m_L and m_R run over interfacial end-atoms of the leads. In general, there are M such atomic positions, defining the perimeter of the tube ends. The number of hybridization contacts between a tube and the bridge range between $M_c = 1$ (single contact case, SC) and $M_c = M$ (multi-contact case, MC). Typical real molecular wires are π-conjugate carbon chains with thyol end groups which in the present treatment are replaced by the linear chain model.

Since the major results we present are not qualitatively affected by the use of more realistic quantum chemical models which take into account the precise structure and properties of the molecular bridge and of the attached leads, we keep the description of our problem at the level of the tight-binding model. In order to highlight the topological properties of tubular leads, we first study the simplest case in which periodic boundary conditions are imposed on semi-infinite square lattice stripes, with the cuts parallel to the lattice bonds. We call this electrode specie square lattice tubes (SLT). In the case of CNT, when the graphene honeycomb lattice is rolled along the lattice bonds such that ℓ hexagons are transversally wrapped, an armchair single wall (ℓ, ℓ) nanotube is obtained, and $M = 2\ell$. According to Eq. (1) CNT are then described at the single-band tight-binding level for π orbitals. This is equivalent to assume that among the four valence carbon orbitals no interaction between the σ (2s and $2p_{x,y}$) and π orbital is significant because of their different symmetries. The fourth electron, a p_z orbital, determines the electronic properties which can be calculated by means of a tight-binding treatment, on the same level as we treat the molecular bridge. There are two such electrons per unit cell in a honeycomb structure, the π and π* band, rendering the electronic properties of the material interesting, i.e. it can be a priori either metallic or semiconducting [28].

We study quantum transport in the framework of the Landauer theory [29] which relates the conductance of the system in the linear response regime to an independent-electron scattering problem [30]. The electron wave function is assumed to extend coherently across the whole device. The two-terminal conductance g at zero temperature is simply proportional to the total transmittance, $T(E_F)$, for injected electrons at the Fermi energy E_F

$$g = \left(2e^2/h\right) T(E_F). \quad (2)$$

The factor 2 accounts for spin degeneracy. The transmission function can be calculated from the knowledge of the molecular energy levels, the

nature and the geometry of the contacts. One can see this by expressing the Green function matrix of the full problem, $G^{-1} = G^{\text{wire}^{-1}} + \Sigma^{\text{L}} + \Sigma^{\text{R}}$, in terms of the bare wire Green function and the self-energy correction due to the presence of the leads. Making use of the Fisher–Lee relation [31] one can finally write

$$T(E) = 4\text{Tr}\{\Delta^{\text{L}}(E)G(E)\Delta^{\text{R}}(E)G^{\dagger}(E)\}, \tag{3}$$

where

$$\Delta^{\alpha}(E) = \frac{\text{i}}{2}\left(\Sigma^{\alpha}(z) - \Sigma^{\alpha^{\dagger}}(z)\right)\Big|_{z=E+\text{i}0^{+}}. \tag{4}$$

For the system under investigation where only the first and last atom of the chain is coupled to the leads, the formula for the transmission simplifies to

$$T(E) = 4\Delta^{\text{L}}(E)\Delta^{\text{R}}(E)|G_{1N}(E)|^2, \tag{5}$$

where the spectral densities Δ^{L} and Δ^{R} are the only non-zero elements $(\Delta^{\text{L}})_{11}$ and $(\Delta^{\text{R}})_{NN}$, respectively, of the matrices Δ. The matrix element $\Delta^{\text{L(R)}}$ is the spectral density of the left (right) lead. It is related to the semi-infinite lead Green function matrix $\mathscr{G}^{\text{L(R)}}$. It is minus the imaginary part of the lead self-energies (per spin),

$$\Sigma^{\alpha} = \Lambda^{\alpha} - \text{i}\Delta^{\alpha} = \sum_{m_{\alpha},m'_{\alpha}} \Gamma_{m_{\alpha}}\Gamma^{*}_{m'_{\alpha}}\mathscr{G}^{\alpha}_{m_{\alpha}m'_{\alpha}}, \tag{6}$$

with $\alpha = \text{L}, \text{R}$. Owing to the causality of self-energy, its real part Λ can be entirely derived from the knowledge of Δ via a Hilbert transform.

The RHS of Eq. (5) coincides with formulas used to describe electron transfer in molecular systems [32]. The above relationship between the Landauer scattering matrix formalism on the one side and transfer hamiltonian approaches on the other side has been worked out in the recent past [11,33] showing de facto their equivalence. This enables us to make use of the formulas from a Bardeen-type picture in terms of spectral densities, which is often convenient for an understanding and analysis of results obtained.

3. Molecular Green function

One has to calculate from the $N \times N$ matrix, $G^{\text{wire}^{-1}} = E + \text{i}0^{+} - H_{\text{wire}}$, the Green function matrix element G_{1N} needed in Eq. (5). This matrix element refers to the two ends of the N-atom-molecule. Its computation requires an $N \times N$ matrix inversion. Since only the molecular-end on-site energies are perturbed by the interaction with the leads via the self-energies Σ^{α}, some general conclusions can already be drawn without an explicit computation of G_{1N}, namely one can write [34]

$$G_{1N} = \frac{G^{\text{wire}}_{1N}}{\left(1 - \Sigma^{\text{L}}G^{\text{wire}}_{11}\right)\left(1 - \Sigma^{\text{R}}G^{\text{wire}}_{NN}\right) - \Sigma^{\text{L}}\Sigma^{\text{R}}\left(G^{\text{wire}}_{1N}\right)^2}. \tag{7}$$

The interaction with the leads dresses, via the self-energy Σ^{α}, the bare molecular wire Green function element G^{wire}_{1N}. The latter can be calculated analytically in the case of a homogeneous wire ($\varepsilon^{\text{wire}}_{n} = \varepsilon^{\text{wire}}$, $\gamma^{\text{wire}}_{\langle n_{\alpha},n'_{\alpha}\rangle} = \gamma^{\text{wire}}$). In fact, upon projecting on the N dimensional molecular wire basis, the determinant of the bare molecular Green matrix factorizes into a dimensionless function of only the number of chain atoms, and of the ratio $\eta^{\text{wire}} = (E - \varepsilon^{\text{wire}})/(2\gamma^{\text{wire}})$. This leads to a closed form for the molecular contribution to the conductance. Namely, one can easily check that $G^{\text{wire}}_{1N} = \gamma^{\text{wire}^{N-1}}\det(G^{\text{wire}}) = (\gamma^{\text{wire}})^{-1}\xi_0/\xi_N$, and $G^{\text{wire}}_{11} = G^{\text{wire}}_{NN} = \gamma^{\text{wire}^{-1}}\xi_{N-1}/\xi_N$, where the exact form of ξ reads:

$$\xi_N(\eta^{\text{wire}}) = \left(\eta^{\text{wire}} + \sqrt{(\eta^{\text{wire}})^2 - 1}\right)^{N+1} - \left(\eta^{\text{wire}} - \sqrt{(\eta^{\text{wire}})^2 - 1}\right)^{N+1}.$$

After some algebra one finds that ξ possesses the recursive property $\xi_N\xi_{N-2} = \xi^2_{N-1} - \xi^2_0$, which leads us to re-write Eq. (7) as

$$\frac{\xi_0}{\gamma^{\text{wire}}G_{1N}} = \xi_N - \left(\frac{\Sigma^{\text{L}}}{\gamma^{\text{wire}}} + \frac{\Sigma^{\text{R}}}{\gamma^{\text{wire}}}\right)\xi_{N-1} + \frac{\Sigma^{\text{L}}\Sigma^{\text{R}}}{\gamma^{\text{wire}^2}}\xi_{N-2}. \tag{8}$$

In other words, the inverse Green function matrix element connecting left and right leads can be written as a sum of terms, representing the inverse of the bare Green function matrix elements for a wire of N, $N-1$, and $N-2$ atoms. In the limit of weak contact coupling, the behavior of the

G_{1N} element is dominated by ξ_N, leading to N transmission resonances in the conductance of unit height. Nevertheless, if the effective coupling between the molecule and the lead is much larger than γ^{wire}, ξ_{N-2} will become the dominant term. As a consequence the conductance spectrum is effectively that of an $(N-2)$-atomic wire [35]. The resonant behavior inside the wire band ($|\eta^{\text{wire}}| \leqslant 1$) and its modification due to the lead coupling is easily understood by writing the transmission as $T = 4\delta^2 \sin^2(\vartheta)/\mathscr{D}$, where the denominator $\mathscr{D}$ takes the following compact exact form valid for all $N \geqslant 1$

$$\mathscr{D} = \big(\sin(N+1)\vartheta - \big(\delta^2 - \lambda^2\big)\sin(N-1)\vartheta - 2\lambda \sin N\vartheta\big)^2 + 4(\delta \sin N\vartheta - \lambda\delta \sin(N-1)\vartheta)^2.$$

Here $\sigma = \lambda - \mathrm{i}\delta = \Sigma/\gamma^{\text{wire}}$ is the self-energy of the leads (for simplicity assumed to be equal) normalized by the wire hopping. The parameter

$$\vartheta = \cos^{-1}\eta^{\text{wire}} = \frac{\mathrm{i}}{2}\ln\frac{\eta^{\text{wire}} - \sqrt{\eta^{\text{wire}^2} - 1}}{\eta^{\text{wire}} + \sqrt{\eta^{\text{wire}^2} - 1}}, \tag{9}$$

is real in the wire band giving rise to resonances for injected electrons matching the wire eigenenergies. Outside the wire band ϑ is pure imaginary (sin functions are effectively sinh functions), and the transmission has a power law dependence on energy and an exponential dependence on the wire length, that is

$$T \sim |2\eta^{\text{wire}}|^{-2N} \quad \text{for } |\eta^{\text{wire}}| \gg 1, \tag{10}$$

in agreement with previous results [36]. This analytic expression for the transmission provides the generalization of existing results [32,33,37] to the case with non-vanishing real part of the self-energies. The density of states $\mathscr{N} = -\mathrm{Im}\,\mathrm{Tr}\{G\}/\pi$ can also be written in a closed analytical form. One can therefore take advantage of the fact that, due to the wire homogeneity, all the diagonal elements except the first and the last one coincide,

$$G_{kk}|_{1<k<N} = \frac{1}{\gamma^{\text{wire}}}\,\frac{\xi_{N-1} - 2\sigma\xi_{N-2} + \sigma^2\xi_{N-3}}{\xi_N - 2\sigma\xi_{N-1} + \sigma^2\xi_{N-2}}.$$

By using parametrization (9) one can easily recast the density of states into the compact form

$$\mathscr{N} = -\frac{1}{\pi\gamma^{\text{wire}}} \times \mathrm{Im}\big\{N\sin N\vartheta - 2(N-1)\sigma\sin(N-1)\vartheta + (N-2)\sigma^2\sin(N-2)\vartheta\big\} / \big\{\sin(N+1)\vartheta - 2\sigma\sin N\vartheta + \sigma^2\sin(N-1)\vartheta\big\}.$$

4. Electrode self-energy

In calculating the spectral function, we make use of the assumption of identical left and right leads and drop the self-energy indices in Eq. (6). Since the Hamiltonian is discrete, we can write the lattice Green function $G = (E + \mathrm{i}0^+ - H)^{-1}$ in matrix form by rearranging the two dimensional n lattice coordinate in Eq. (1). We assume the x direction to be parallel to the tubes (and to the transport direction) and y to be the finite transverse coordinate (see Fig. 1). The latter is curvilinear with n_y spanning M sites with periodic boundary conditions.

The lattice representation of the lead Green function is needed in the calculation of the self-energy contribution. It can generally be written by projecting the Green operator onto the localized state basis, $\psi_{k_x,k_y}(n_x = \text{border}, n_y) = \chi_{k_x}\phi_{k_y}(n_y)$, of the semi-infinite lead

$$\mathscr{G}_{n_y n_y'}(E) = \left\langle n_y \middle| \big(E + \mathrm{i}0^+ - H\big)^{-1} \middle| n_y' \right\rangle = \sum_{k_x,k_y} \frac{\chi_{k_x}\phi_{k_y}(n_y)\chi^*_{k_x}\phi^*_{k_y}(n_y')}{E + \mathrm{i}0^+ - E_{k_x,k_y}}. \tag{11}$$

4.1. One-dimensional electrodes: Newns model

We first recall the particular case of linear chain electrodes (onto which we will map our system due to the validity of a channel selection). For such a simple model the dispersion relation as a function of the lattice on-site energies ε, of the hopping terms γ, and of the lattice spacing a is simply given by $E = \varepsilon - 2\gamma\cos k_x a$. As a result the surface Green function for the semi-infinite chain is obtained by inserting the wave function at the lead origin $\chi_{k_x} = \sqrt{2/\pi}\sin k_x a$ in the defining expression (11) and transforming the only sum over momenta into an integral, due to the infinite system size. Thus,

$$\mathcal{G}(E) = \frac{a}{\pi}\int_{-\pi/a}^{\pi/a} \mathrm{d}k_x \frac{\sin^2 k_x a}{E + \mathrm{i}0^+ - \varepsilon + 2\gamma\cos k_x a} = \frac{\mathrm{e}^{\mathrm{i}k_x(E)a}}{-\gamma},$$

where we solved the integral according to Brodovitsky [38] and we made use of the dispersion relation. The resulting spectral density, given by Eq. (6), is the semi-elliptical local density of states (LDOS) as obtained by Newns in his theory of chemisorption [39]

$$\Delta^{\mathrm{Newns}}(\eta) = \frac{\Gamma_{\mathrm{eff}}^2}{\gamma}\sqrt{1-\eta^2}\Theta(1-|\eta|).$$

Γ_{eff} is the strength of the single contact between the molecule and the semi-infinite one-dimensional leads, $\eta = (E-\varepsilon)/(2\gamma)$ is the band-normalized energy, and Θ the Heaviside function. The real part of the self-energy, responsible for shifting the molecular resonances, is simply proportional to $\cos k_x a$ and thus linear in energy. Its full dependence on energy is given by Hilbert transforming Δ, and it reads

$$\mathrm{Re}\Sigma = \frac{\Gamma_{\mathrm{eff}}^2}{\gamma} \times \left(\eta - \sqrt{\eta^2-1}(\Theta(\eta-1) - \Theta(-\eta-1))\right).$$

4.2. Square lattice tubular electrodes

Square lattice leads are characterized by periodic boundary conditions perpendicularly to the lead direction. Transverse momentum quantization leads to $k_y^j a = 2\pi j/M$ (with $0 \leqslant j < M$). The surface Green function for such a system can be written as

$$\mathcal{G}_{n_y n_y'}(E) = \frac{a}{\pi M}\sum_{k_y}\int_{-\pi/a}^{\pi/a}\mathrm{d}k_x \times \frac{\sin^2(k_x a)\varphi_j(n_y)\varphi_j^*(n_y'),}{E + \mathrm{i}0^+ - \varepsilon + 2\gamma\cos k_y a + 2\gamma\cos k_x a} = \frac{1}{M}\sum_{j=0}^{M-1}\varphi_j(n_y)\tilde{G}^j(E)\varphi_j^*(n_y'), \quad (12)$$

where $\tilde{G}^j(E) = -\mathrm{e}^{\mathrm{i}k_x^j(E)a}/\gamma$ has been obtained by solving an integral formally equivalent to the linear chain case and using the dispersion relation

$$E = \varepsilon - 2\gamma\left(\cos k_y^j a + \cos k_x^j(E)a\right). \quad (13)$$

The transverse profile of the wave function is given by $\varphi_j(n_y) = \exp(\mathrm{i}k_y^j n_y a)$. Note that the wave function is obtained by a further normalization, namely $\phi = \varphi/(Ma)^{1/2}$.

The self-energy finally reads as a sum of weighted longitudinal wave function profiles

$$\Sigma = \frac{1}{M}\sum_{j=0}^{M-1}\tilde{G}^j(E)\eta_{j/M}[\Gamma],$$

where the weight

$$\eta_{j/M}[\Gamma] = \left|\sum_{m=0}^{M-1}\Gamma_m\varphi_j(m)\right|^2 \quad (14)$$

is the contact-averaged transverse wave function. Depending on the contact geometry one has to specify the distribution of the Γ_m contacts to calculate the weight η and thus the self-energy. Note that $\eta_{(\cdot)}$ is formally the square modulus of the Fourier series of $\Gamma_{(\cdot)}$; thus the zero-mode transverse momentum state $j = 0$ contributes to η with the square of the mean contact strength. Due to the geometry of the lead surface, it is reasonable to assume a uniform distribution of contacts between the molecular wire and the electrodes. For contacts of equal strength $\Gamma_m = \Gamma_{\mathrm{eff}}/\sqrt{M_{\mathrm{c}}}$, active on $M_{\mathrm{c}} \leqslant M$ sites, we obtain a modulation for the contributing channels governed by

$$\eta_{j/M}(\Gamma_{\mathrm{eff}}, M_{\mathrm{c}}) = \Gamma_{\mathrm{eff}}^2 M_{\mathrm{c}}\frac{\mathrm{sinc}^2(\pi j M_{\mathrm{c}}/M)}{\mathrm{sinc}^2(\pi j/M)},$$

where $\mathrm{sinc}(x \neq 0) \equiv \sin(x)/x$, and $\mathrm{sinc}(x = 0) \equiv 1$. One can decompose the spectral density into a sum over the spectral densities of each state j. Namely $\Delta = \Delta^{(0)}\sum_j w_j(E)$, with $\Delta^{(0)} = \Gamma_{\mathrm{eff}}^2 M_{\mathrm{c}}/(\gamma M)$. The channel weights are obviously independent upon rotation of the interfacial coupling position as Σ itself is.

In Fig. 2, the weights $w_j(E)$ are visualized for different contact values $1 \leqslant M_{\mathrm{c}} \leqslant 6$.

For the case $M = M_{\mathrm{c}}$ the contributions from all states are suppressed except the state with zero

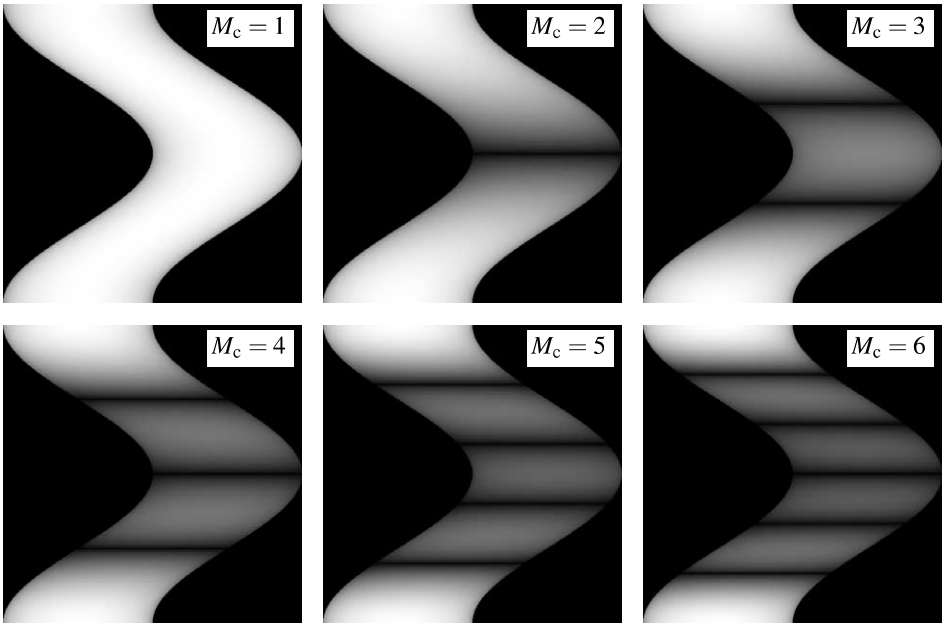

Fig. 2. Spectral weights $w_j(E)$ plotted for different contact values M_c; a non-linear grey level scale is used with black corresponding to 0 and white to 1; small weights are amplified for better visualization. In every panel the horizontal axis represents the normalized energy $-2 \leqslant (E-\varepsilon)/(2\gamma) \leqslant 2$, and the vertical axis the normalized wave number $0 \leqslant j/M < 1$. Note that in the mesoscopic limit, $M_c/M \lesssim 1$, the states $j \neq 0$ match the nodes of $\Delta_j(E)$: only the zero-transverse momentum $j = 0$ contributes to transport.

transverse momentum, which is the outcome of the sum rule (14). That is, $\eta = \Gamma_{\mathrm{eff}}^2 M \delta_{j,0}$. Thus the configuration with all contacts of the tube ends coupled to the molecule with strength $\Gamma_{\mathrm{eff}}/\sqrt{M}$ is equivalent to the case of a single contact with strength Γ_{eff} to a one-dimensional lead (previous section). Moreover a scaling law is found for Σ, and a fortiori for the conductance given by $g = g(\bar{\Gamma}\sqrt{M_c})$, where $\bar{\Gamma}$ is the local contact strength.

In Fig. 3, Δ is displayed as a function of energy, lead diameters and active contacts. As easily visible, it is only for values M_c of the order of the available contacts M that the mesoscopic nature of the scattering channels enter the spectral density. The larger the tube diameter the lower is the number of contacts which are needed to reach a MC-like spectral density. This observation justifies the use of the one-dimensional Newns model for leads of lateral dimension much larger than the contacted molecule but also shows the limit of this approach when dealing with quasi-one-dimensional leads. It remains to investigate to which extent the results obtained so far can be generalized to realistic quasi-one-dimensional structures such as CNT.

4.3. CNT electrodes

When the armchair (ℓ, ℓ) CNT topology is imposed the number of carbon sites at the interface is $M = 2\ell$. The eigenvalues of the tight-binding hamiltonian (1),

$$E_{\pm}(k_x^j, j) = \varepsilon \pm \gamma \sqrt{1 + 4\cos\left(\frac{j\pi}{\ell}\right)\cos\left(\frac{k_x^j a}{2}\right) + 4\cos^2\left(\frac{k_x^j a}{2}\right)}, \tag{15}$$

are obtained in a basis set given by symmetric (+) and antisymmetric (−) site configurations of the graphene bipartite lattice, corresponding to π and π^* orbitals respectively, [28,40]. The longitudinal momentum is restricted to the Brillouin zone, $-\pi < k_x^j a < \pi$, and the transverse wave number $1 \leqslant j \leqslant 2\ell$ labels 4ℓ bands, as many as the number

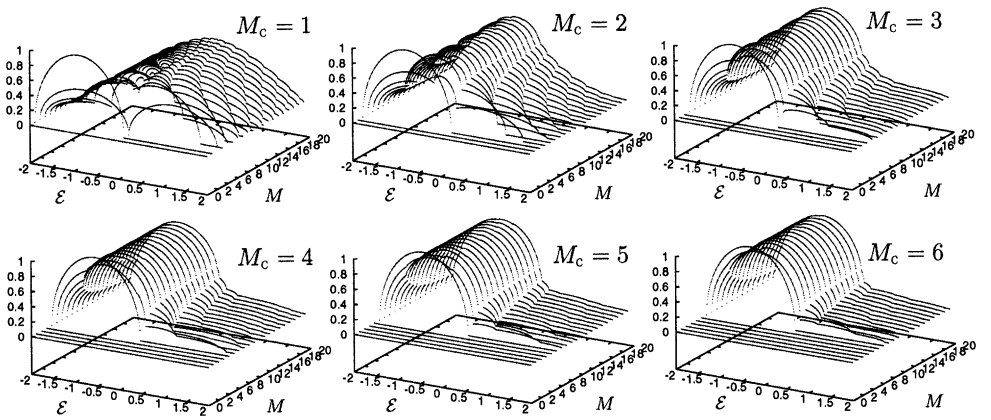

Fig. 3. The normalized spectral density $\Delta\gamma/\Gamma_{\rm eff}^2$ plotted for different maximum values M_c as in Fig. 2; the x-axis represent the normalized energies $-2 \leqslant (E-\varepsilon)/(2\gamma) \leqslant 2$, the y-axis label the dimensionality of the leads (number of possible contacts) $M_c \leqslant M \leqslant 20$.

of atoms in the unit cell of a (ℓ,ℓ) CNT. The two bands corresponding to $j = \ell$ are singly degenerate. They are responsible for the metallic character of armchair CNTs (these two bands cross at the Fermi level $E = \varepsilon$ for $k_x^\ell a = \pm 2\pi/3$). Also the two outermost bands corresponding to $j = 2\ell$ are singly degenerate while the other remaining $(4\ell - 4)$ bands are collected in $(2\ell - 2)$ doubly degenerate dispersion curves.

The single-particle Green function in a lattice representation for two sites belonging to the same sub-lattice can be still written as in Eq. (12) as

$$\mathcal{G}_{n_y,n'_y}(E) = \frac{1}{2\ell}\sum_{j=1}^{2\ell}\varphi_j(n_y)\tilde{G}^j(E)\varphi_j^*(n'_y), \tag{16}$$

where $\varphi_j(n_y) = \exp(\mathrm{i}k_y^j n_y^j a)$, with $k_y^j a = \pi j/\ell$, and $1 \leqslant j \leqslant 2\ell$. Note that in Eq. (16), n_y and n'_y should be either even or odd (that is they should belong to the same sublattice). The semi-infinite longitudinal Green function is given by

$$\tilde{G}^j(E) = \frac{a}{8\pi}\sum_{\beta=\pm}\int_{-\pi/a}^{\pi/a}\mathrm{d}k_x^j\frac{\sin^2\left(k_x^j a/2\right)}{E + \mathrm{i}0^+ - E_\beta\left(k_x^j, j\right)}.$$

The integral can be worked out analytically by extending k_x^j to the complex plane and adding cross-cancelling paths (parallel to the imaginary axis) along the semi-infinite rectangle in the half plane $\mathrm{Im}\,k_x^j > 0$ and based on the interval between $-\pi/a$ and π/a. The closing path parallel to the real axis gives a real contribution linear in energy. This generalizes the approach by Ferreira et al. [41], recently adopted for obtaining an analytical expression for the diagonal Green function of infinite achiral tubes, to the case of semi-infinite CNTs. The determination of the poles inside the integration contour, given by

$$\cos\left(\frac{q_\beta^j a}{2}\right) = -\frac{1}{2}\cos\left(\frac{j\pi}{\ell}\right) - \frac{\beta}{2}\sqrt{\left(\frac{E-\varepsilon}{2\gamma}\right)^2 - \sin^2\left(\frac{j\pi}{\ell}\right)}$$

allows for the calculation of the residues and thus of the surface Green function. One finds

$$\tilde{G}^j\left(E\right) = \frac{1}{2\gamma}\frac{E-\varepsilon}{2\gamma}\left(\frac{1}{2} + \mathrm{i}\sin\left(\frac{q_{\beta_*}^j a}{2}\right)\Big/\sqrt{\left(\frac{E-\varepsilon}{2\gamma}\right)^2 - \sin^2\left(\frac{j\pi}{\ell}\right)}\right), \tag{17}$$

where the choice of the contributing pole through the branch parameter $\beta_* = \mathrm{sign}\,(E-\varepsilon)$ has to be taken into account. The LDOS, obtained from the imaginary part of the surface Green function after Eq. (17) is plugged into Eq. (16), is shown in Fig. 4. It clearly differs from the LDOS of an infinite CNT as depicted for comparison in the right panel. As for the case of the SLT the pinning of the longitudinal wave function at the surface of the semi-infinite systems *cancels* all border zone anomalies

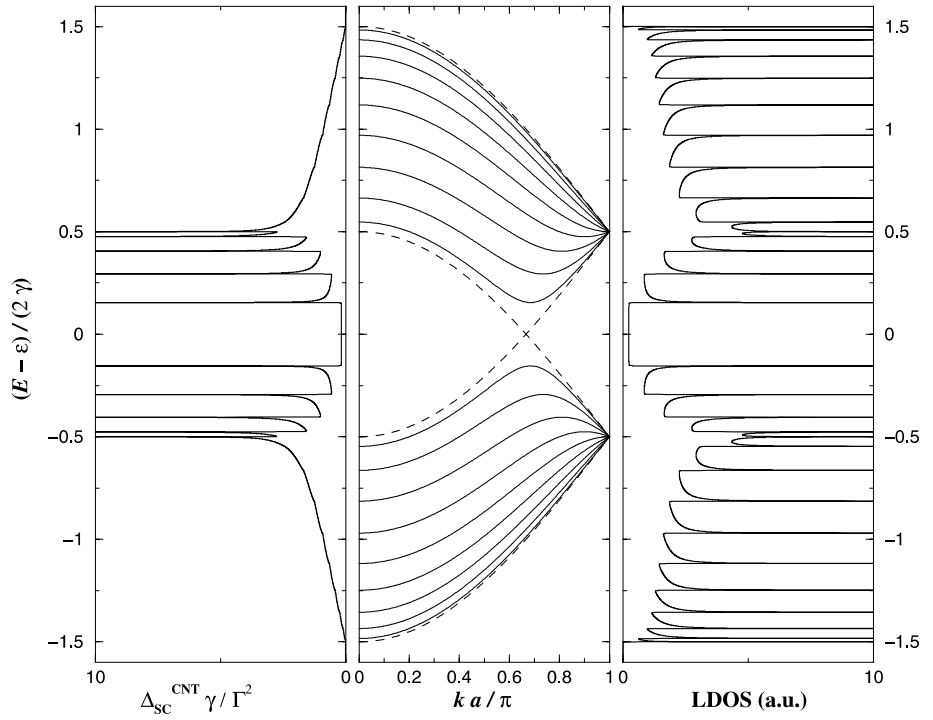

Fig. 4. Left panel: the normalized spectral density for a semi-infinite (ℓ,ℓ) CNT lead in the SC configuration; it corresponds to the LDOS at any atom site at the cut of the CNT lead. For comparison the dispersion relation and the LDOS of an infinite (ℓ,ℓ) CNT are shown in the middle and right panel, respectively. Solid lines in the dispersion relation panel indicate doubly degenerate bands, dashed lines singly degenerate bands. Here $\ell = 10$, and on-site energies and hopping terms refer to $\alpha = \mathrm{L},\mathrm{R}$-leads.

when $q_{\pm}^{j}a$ matches multiples of 2π. In infinite SLTs these states are the *only* resonant states (van Hove singularities) so that the surface LDOS of a semi-infinite SLT never diverges (as it is shown in the left panel of Fig. 5). On the contrary, in CNTs there are states with zero group velocity outside the border zone which are responsible for the singularities of the spectral density of semi-infinite CNTs (left panel of Fig. 4).

The self-energy for a CNT lead is more complicate than the one for a SLT owing to the missing equivalence of the sites belonging to the

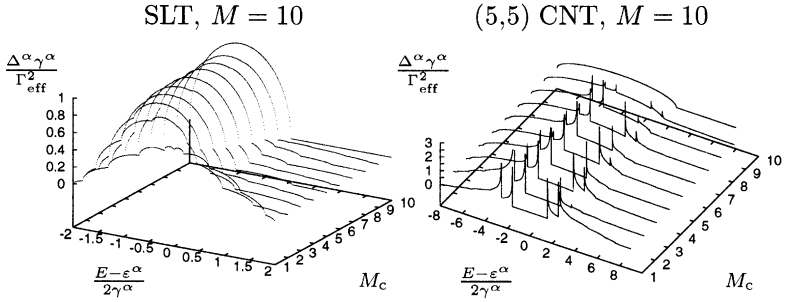

Fig. 5. The normalized spectral density as a function of energy and active contacts is plotted for $M = 10$ possible atomic contacts available; on-site energies and hopping terms refer to $\alpha = \mathrm{L},\mathrm{R}$-leads. The right panel illustrate numerical results after [42] in full agreement with the analytics showed in the text.

two different sub-lattices. However, since the longitudinal part of the Green function, Eq. (17), is the same for all diagonal and off-diagonal terms of the surface Green function, the self-energy can still be cast into the form

$$\Sigma = \frac{1}{2\ell}\sum_{j=1}^{2\ell} \tilde{G}^{j}(E)\eta_{j/\ell}[\Gamma].$$

However, for the calculation of

$$\eta_{j/\ell}[\Gamma] = \left|\sum_{m=1}^{2\ell} \Gamma_m \varphi_j(m)\right|^2, \tag{18}$$

one has to specify the sub-lattice components of the transverse wave function and whether they belong to a bonding or anti-bonding molecular state. Again the distribution of the Γ_m contacts is needed in order to calculate the weight η and thus the self-energy. Eq. (18) simplifies considerably in the SC case: $\eta = \Gamma^2$. Since η is uniform in j the self-energy is simply proportional to the diagonal semi-infinite Green function and, as a consequence, the spectral density is proportional to the local density of states (Fig. 4). The MC case ($\Gamma_m = \Gamma_{\mathrm{eff}}/\sqrt{2\ell}$) is also easily tractable leading to a sum rule over the possible conducting channels. However a direct proof is provided by the intuitive consideration that only the π-bonding state can contribute to the MC spectral density (all the other states have a non-constant spatial modulation provided e.g. in [43]). Following our notation the π-bonding state corresponds to $j = \ell$. Fig. 5 shows the spectral density in the intermediate regime between the SC and MC limits. The two different lead lattice structures carry the same physical information only in the MC limit case.

5. Discussion and concluding remarks

It is interesting to recollect the results for the MC-spectral density, Δ_{MC}, in all three lead models considered so far. Using the dispersion relation (13) and the surface Green function in Eq. (12) the spectral density for SLT leads coincides formally with the Newns LDOS with an energy shift $\Delta_{\mathrm{MC}}^{\mathrm{SLT}}(\eta) = \Delta^{\mathrm{Newns}}(\eta + 1)$. For CNTs Eqs. (15)–(17) lead to $\Delta_{\mathrm{MC}}^{\mathrm{CNT}}(\eta) = \Delta^{\mathrm{Newns}}(\eta + \frac{1}{2})$. From the above discussion it is clear that the multiple contact configuration suppresses features associated with the two-dimensional character of tubular leads, apart from an energy shift. In our model, the latter is the only remnant the system preserves from the transverse momentum component.

In contrast, the SC case is strongly dependent on the lead underlying structure. The spectral density for a single contact, Δ_{SC}, reduces to the LDOS in the lead at the point where the molecular wire is contacted with strength Γ,

$$\Delta_{\mathrm{SC}} = \pi\Gamma^2 \mathrm{LDOS}.$$

It is, in particular, in the SC scenario that the conductance of the molecular wire might be strongly affected by the nature of the leads [35]. Nevertheless, once the nature of the contact can be inferred, one can think to cure the spurious insertion in the conductance by filtering out the contribution of the leads from the molecular resonances. For instance, in the CNT-enhanced STM tips [22] the improved resolution images can be cleaned by de-convolving them using model assumptions for the leads and their contact geometry.

Another significant consequence of the peculiar contact dependence of the spectral density is the possibility to understand the influence of the mesoscopic character of the leads. In the limit of large M (at fixed M_{c}), η looses its granularity being sampled by many more states compared to its nodes, whereas for $M_{\mathrm{c}}/M \lesssim 1$ an increasing number of nodes matches the decreasing number of states. This determines a reduction in the self-energy, and thus in the width of the molecular resonances, highlighting the quantum features of the wire. The latter result in a quite striking behavior for CNTs because of the band anomalies outside of the border zone which strongly determine the resonant behavior of the spectral density.

To conclude, we have shown that novel features are expected to arise in the conductance of a molecular wire connected to nanotube leads. The commonly used approximation of a pure imaginary, flat, wide band self-energy is not valid when employing tubular leads. Nevertheless, the conductance of a homogeneous molecular wire still possesses an analytical form in the entire regime of

the wire parameters and allows for the insertions of a non-vanishing real self-energy, necessarily arising when considering nanotube leads. By tailoring the geometry and dimensionality of the contacts, it is possible to perform a channel selection. In the MC limit the conductance becomes independent of the lattice structure of the tubular electrodes, transport is dominated by topology properties and is effectively one-dimensional. Furthermore, the conductance obeys a universal scaling law in the multiple contact configuration. We would further like to stress that the derived analytical expression for the semi-infinite CNT self-energy allows for a full analytical treatment of the linear conductance problem. The possibility to handle an exact expression of the semi-infinite CNT Green function may serve as a first step in analytical treatments of more complex carbon-based molecular structures such as T- or Y-junctions [44].

Acknowledgements

Fruitful discussions and valuable correspondence with M.S. Ferreira are gratefully acknowledged. R. Gutiérrez and H.-S. Sim provided perceptive comments to this manuscript. GC research at MPI is sponsored by the Schloeßmann Foundation. GF acknowledges support from the Alexander von Humboldt Foundation.

References

[1] Y. Taur, Proc. IEEE 85 (1997) 4.
[2] B. Crone, A. Dodabalapur, Y. Lin, R.W. Filas, Z. Bao, A. Laduca, R. Sarpeshkar, H.E. Katz, W. Li, Nature 403 (2000) 521;
J.H. Schön, C. Kloc, E. Bucher, B. Batlogg, Nature 403 (2000) 408;
K. Ziemelis, Nature 394 (1998) 619;
J.M. Tour, Chem. Rev. 96 (1996) 537.
[3] J.C. Ellenbogen, J.C. Love, Proc. IEEE 88 (2000) 386.
[4] J.M. Tour, M. Kozaki, J.M. Seminario, J. Am. Chem. Soc. 120 (1998) 8486.
[5] D. Goldhaber-Gordon, M.S. Montemerlo, J.C. Love, G.J. Opiteck, J.C. Ellenbogen, Proc. IEEE 85 (1997) 521.
[6] R. Landauer, IEEE Trans. Electron Devices 43 (1996) 1637.
[7] A. Aviram, M.A. Ratner, Chem. Phys. Lett. 29 (1974) 277.
[8] D.H. Waldeck, D.N. Beratan, Science 261 (1993) 576;
A.S. Martin, J.R. Sambles, G.J. Ashwell, Phys. Rev. Lett. 70 (1993) 218.
[9] M.A. Reed, C. Zhou, C.J. Muller, T.P. Burgin, J.M. Tour, Science 278 (1997) 252.
[10] D. Porath, A. Bezryadin, S. de Vries, C. Dekker, Nature 403 (2000) 635.
[11] A. Nitzan, Ann. Rev. Phys. Chem. 52 (2001) 681.
[12] J. Reichert, R. Ochs, D. Beckmann, H.B. Weber, M. Mayor, H. Löhneysen, Phys. Rev. Lett., cond-mat/0106219, in press.
[13] J.M. van Ruitenbeek, Naturwissenschaften 88 (2001) 59.
[14] A.I. Yanson, G. Rubio Bollinger, H.E. van den Brom, N. Agraït, J.M. van Ruitenbeek, Nature 395 (1998) 783.
[15] H. Ohnishi, Y. Kondo, K. Takayanagi, Nature 395 (1998) 780.
[16] A. Karlsson, R. Karlsson, M. Karlsson, A. Cans, A. Strömberg, F. Ryttsén, O. Orwar, Nature 409 (2001) 150.
[17] T. Rueckes, K. Kim, E. Joselevich, G.Y. Tseng, C.-L. Cheung, C.M. Lieber, Science 289 (2000) 94;
N. Yoneya, E. Watanabe, K. Tsukagoshi, Y. Aoyagi, Appl. Phys. Lett. 79 (2001) 1465.
[18] R. Saito, G. Dresselhaus, M.S. Dresselhaus, Physical Properties of Carbon Nanotubes, World Scientific Publishing, London, 1998;
P. McEuen, Phys. World 13 (2000) 31.
[19] C. Thelander, M.H. Magnusson, K. Deppert, L. Samuelson, P. Rugaard Poulsen, J. Nygård, J. Borggreen, Appl. Phys. Lett. 79 (2001) 2106.
[20] J. Hu, M. Ouyang, P. Yang, C.M. Lieber, Nature 399 (1999) 48;
P.J. de Pablo, E. Graugnard, B. Walsh, R.P. Andres, S. Datta, R. Reifenberger, Appl. Phys. Lett. 74 (1999) 323.
[21] V. Derycke, R. Martel, J. Appenzeller, Ph. Avouris, Nano Lett. 1 (2001) 453;
H.W.C. Postma, T. Teepen, Z. Yao, M. Grifoni, C. Dekker, Science 293 (2001) 76;
R. Martel, T. Schmidt, H.R. Shea, T. Hertel, Ph. Avouris, Appl. Phys. Lett. 73 (1998) 2447.
[22] H. Watanabe, C. Manabe, T. Shigematsu, M. Shimizu, Appl. Phys. Lett. 78 (2001) 2928.
[23] S.S. Wong, E. Joselevich, A.T. Woolley, C.L. Cheung, C.M. Lieber, Nature 394 (1998) 52.
[24] H. Nishijima, S. Kamo, S. Akita, Y. Nakayama, K.I. Hohmura, S.H. Yoshimura, K. Takeyasu, Appl. Phys. Lett. 74 (2000) 4061.
[25] S. Akita, H. Nishijima, T. Kishida, Y. Nakayama, Jpn. J. Appl. Phys. 39 (2000) 7086;
A.I. Onipko, K.-F. Berggren, Y.O. Klymenko, L.I. Malysheva, J.J.W.M. Rosink, L.J. Geerligs, E. van der Drift, S. Radelaar, Phys. Rev. B 61 (2000) 11118;
A.L. Vázquez de Parga, O.S. Hernán, R. Miranda, A. Levy Yeyati, N. Mingo, A. Martín-Rodero, F. Flores, Phys. Rev. Lett. 80 (1998) 357.
[26] G. Cuniberti, R. Gutiérrez, G. Fagas, F. Großmann, K. Richter, R. Schmidt, Physica E 12 (2002) 749;

R. Gutiérrez, G. Fagas, G. Cuniberti, F. Großmann, R. Schmidt, K. Richter, Phys. Rev. B 65 (2002) 113410.
[27] N.D. Lang, Ph. Avouris, Phys. Rev. Lett. 84 (2000) 358.
[28] R. Saito, M. Fujita, G. Dresselhaus, M.S. Dresselhaus, Phys. Rev. B 46 (1992) 1804.
[29] Y. Imry, R. Landauer, Rev. Mod. Phys. 71 (1999) S306.
[30] D.K. Ferry, S.M. Goodnick, Transport in Nanostructures, vol. 6, Cambridge Studies in Semiconductor Physics and Microelectronic Engineering, Cambridge University Press, Cambridge, 1999.
[31] D.S. Fisher, P.A. Lee, Phys. Rev. B 23 (1981) R6851.
[32] V. Mujica, M. Kemp, M.A. Ratner, J. Chem. Phys. 101 (1994) 6849;
V. Mujica, M. Kemp, M.A. Ratner, J. Chem. Phys. 101 (1994) 6856.
[33] L.E. Hall, J.R. Reimers, N.S. Hush, K. Silverbrook, J. Chem. Phys. 112 (2000) 1510.
[34] S.S. Skourtis, J.N. Onuchic, Chem. Phys. Lett. 209 (1993) 171.
[35] G. Fagas, G. Cuniberti, K. Richter, Phys. Rev. B 63 (2001) 045416.
[36] H.M. McConnell, J. Chem. Phys. 35 (1961) 508.
[37] M. Sumetskii, J. Phys.: Condens. Matter 3 (1991) 2651;
V.V. Malov, L.V. Iogansen, Opt. Spektrosk. (USSR) 48 (1980) 146.
[38] K.V. Brodovitsky, Doklady Akademii NAUK SSSR 120 (1958) 1178;
See also eq. 3.644.4 in I.S. Gradschteyn, I.M. Ryzhik, Tables of Integrals, Series and Products, sixth ed., Academic Press, San Diego, 2000.
[39] D.M. Newns, Phys. Rev. 178 (1969) 1123.
[40] P.R. Wallace, Phys. Rev. 71 (1947) 622.
[41] M.S. Ferreira, T.G. Dargam, R.B. Muniz, A. Latgé, Phys. Rev. B 63 (2001) 245111, this reference contains some misprints, especially in the final diagonal form of the Green function of an infinite CNT amended in the erratum, Phys. Rev. B 65 (2002) 039901.
[42] G. Cuniberti, G. Fagas, K. Richter, Acta Phys. Pol. 32 (2001) 437.
[43] H.J. Choi, J. Ihm, Solid State Commun. 111 (1999) 385.
[44] L.-M. Peng, Z.L. Zhang, Z.Q. Xue, Q.D. Wu, Z.N. Gu, D.G. Pettifor, Phys. Rev. Lett. 85 (15) (2000) 3249;
C. Papadopoulos, A. Rakitin, J. Li, A.S. Vedeneev, J.M. Xu, Phys. Rev. Lett. 85 (16) (2000) 3476.